Three-dimensional time-dependent quantum mechanical study of the reaction He + H$_2^+$ → HeH$^+$ + H

N BALAKRISHNAN and N SATHYAMURTHY*

Department of Chemistry, Indian Institute of Technology, Kanpur 208 016, India

Abstract. We report the results of a three-dimensional time-dependent quantum mechanical study of the reaction He + H$_2^+$ ($v = 0, 1$) → HeH$^+$ + H at $\langle E_{trans} \rangle = 1 \cdot 0$ eV, which reproduces clearly the vibrational enhancement for the system. In addition, preliminary results for He + HD$^+$ ($v = 1$–3) suggest the preferential formation of HeD$^+$ over HeH$^+$ in the products.

Keywords. Time-dependent quantum mechanics; vibrational enhancement; isotopic branching.

1. Introduction

Recent years have witnessed significant advances in the development of the time-dependent quantum mechanical (TDQM) method as a viable tool for investigating atomic and molecular collisions (Gerber *et al* 1986; Kosloff 1988; Mohan and Sathyamurthy 1988; Kulander 1991). However, progress towards three-dimensional (3D) study of reactive scattering has been rather limited (Judson *et al* 1990; Neuhauser *et al* 1990). Difficulties in methodology arise because of the presence of multiple arrangement channels and the usual Jacobi coordinates for inelastic scattering are not the most suited for modelling reactive scattering events. Hyperspherical coordinates (Smith 1962; Whitten and Smith 1968; Kuppermann 1975) have proved to be quite successful in describing reactive collisions as all arrangement channels are represented evenhandedly in this system. In this communication, we present the results of a 3D TDQM study of the reaction

$$\text{He} + \text{H}_2^+ \rightarrow \text{HeH}^+ + \text{H}$$
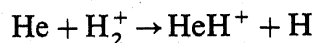
on the chemically accurate McLaughlin–Thompson–Joseph–Sathyamurthy (McLaughlin and Thompson 1979; Joseph and Sathyamurthy 1987) (MTJS) *ab initio* potential energy surface (PES) for zero total angular momentum ($J = 0$) collisions in hyperspherical coordinates.

2. Methodology

The hyperspherical coordinates used in the present study are a slightly modified version of Johnson's hyperspherical coordinates (Johnson 1980), as used by Muckerman

---

et al (1988). These consist of three internal coordinates (ρ, θ, ϕ) and three external coordinates (α, β, γ) which are the three Euler angles. The potential energy of the system is a function of only the internal coordinates. The hyper-radius, ρ, represents the overall size of the system, θ is a bending angle, and ϕ, the kinematic angle represents the arrangement channel. Their ranges of variation are: $0 < \rho < \infty$, $0 \leqslant \theta \leqslant \pi/2$ and $0 \leqslant \phi \leqslant 2\pi$. For the special case of $J = 0$ collisions, the Hamiltonian contains only the internal coordinates. It can be written after a proper transformation of the wavefunction (Muckerman *et al* 1988) as

$$\hat{H} = -\frac{\hbar^2}{2\mu}\frac{\partial^2}{\partial\rho^2} + \hat{H}_1, \tag{1}$$

where

$$\hat{H}_1 = -\frac{\hbar^2}{2\mu}\left[\frac{\partial^2}{\partial\theta^2} + \frac{1}{\sin^2\theta}\frac{\partial^2}{\partial\phi^2} + \frac{1}{\rho^2}\left(\frac{1}{4} + \frac{4}{\sin^2 2\theta}\right)\right] + V(\rho, \theta, \phi). \tag{2}$$

The initial wavefunction, at time $t = 0$, required for solving the time-dependent Schrödinger equation

$$\hat{H}\Psi = i\hbar\frac{\partial\Psi}{\partial t} \tag{3}$$

was set up on a (ρ, θ, ϕ) grid as

$$\Psi(\rho, \theta, \phi) = F(\rho)\Phi(\theta, \phi; \rho), \tag{4}$$

where $F(\rho)$ was taken to be a minimum uncertainty Gaussian wavepacket and $\Phi(\theta, \phi; \rho)$ was initialized as an asymptotic eigenfunction to $\hat{H}_1$ (Muckerman *et al* 1988). That is, in the limit $\rho \to \infty$, $\Phi(\theta, \phi; \rho)$ is the vib-rotational wavefunction,

$$\psi_{v,j}(x, \eta) = [X_v(x)/x^{1/2}]P_j(\eta), \tag{5}$$

where $X_v(x)$ is a Morse oscillator eigenfunction for the vth vibrational state and $P_j(\eta)$ a Legendre polynomial for the jth rotational state. The variables x and η are expressed in terms of θ and ϕ through the asymptotic relations (Muckerman *et al* 1988; Marković *et al* 1990; Marković and Billing 1992a)

$$\theta = \theta_0 + (x/\rho)\sin\eta, \tag{6a}$$

and

$$\phi = \phi_0 + (x/\rho)\cos\eta, \tag{6b}$$

with $\theta_0 = \pi/2$, which is the same for all the channels. ϕ_0 is different for the different arrangement channels which are obtained by a kinematic rotation along ϕ. The hyperspherical coordinates used in the present study are especially suited to A + B$_2$ systems as a unique diatomic origin occurs at $\phi = \phi_0 = \pi$ with the two other diatomic origins symmetrically located on either side of it at $\phi = \pi \pm \xi$, where $\xi = 2\tan^{-1}(m_B/\mu)$ with m_B the mass of the atom B and μ the three-body reduced mass. For the present system, the He + H$_2^+$ channel is situated at $\phi = 180°$, and the two HeH$^+$ + H channels at $\phi = 281\cdot61°$ and $\phi = 78\cdot39°$.

The different channel locations are illustrated with the aid of potential-energy contours in (θ, ϕ) coordinates for different values of ρ in figure 1.
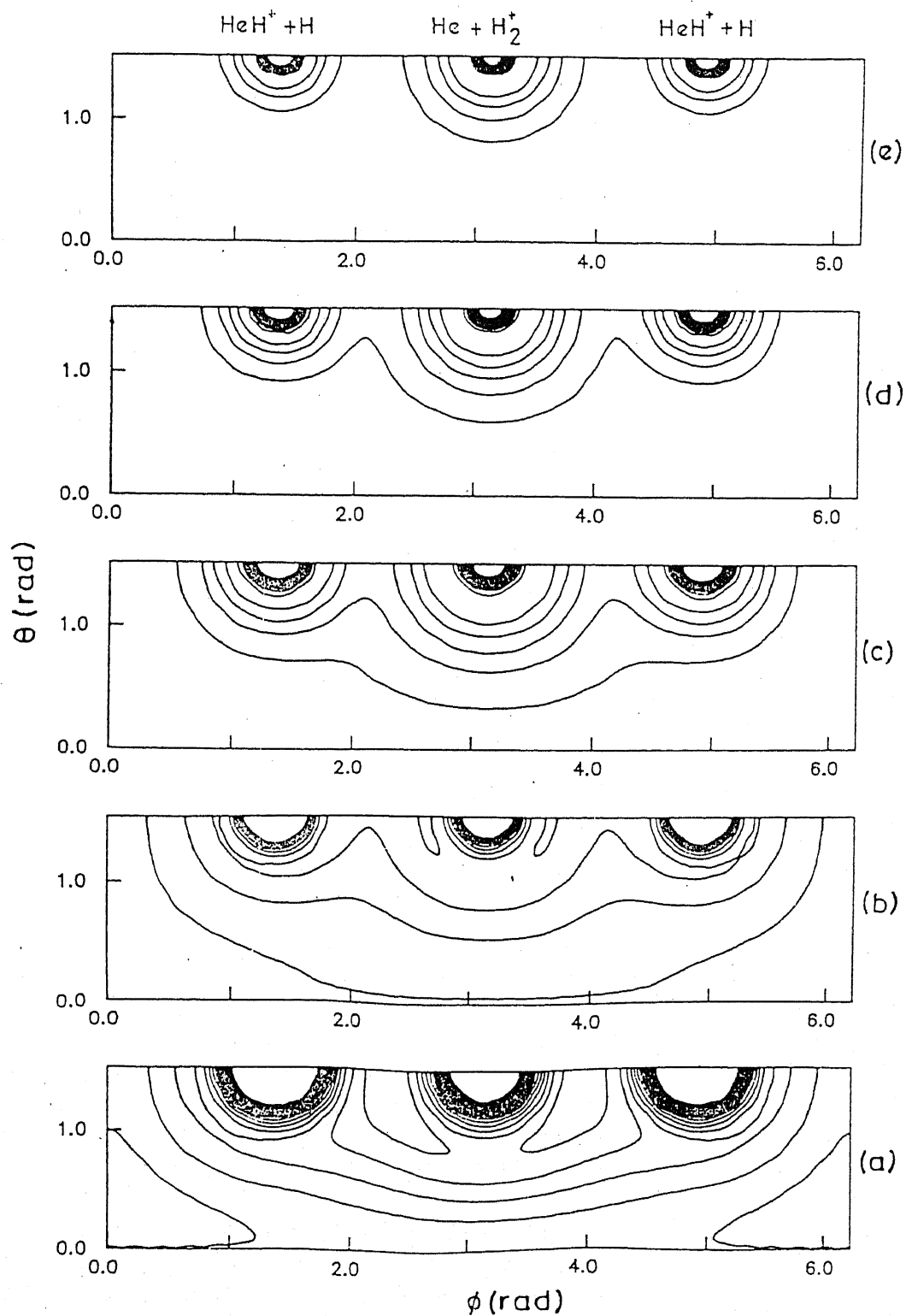
Figure 1. Potential-energy contours for the HeH_2^+ system in (θ, ϕ) space for different values of the hyper-radius $\rho = 4$, 6, 8, 10 and 12 a.u. in (a)–(e) respectively.

A $(128, 32, 64)$ grid was used to discretize the wavefunction in (ρ, θ, ϕ) with $\rho = 2(0.14)19.78$ a.u., and $\phi = 0(\pi/32)2\pi$. The grid along θ needed special attention as the Hamiltonian, $\hat{H}$, is singular at $\theta = 0$ and $\theta = \pi/2$. The singularity at $\theta = 0$ was more problematic because of the $1/\sin^2\theta$ term in the Hamiltonian which contributes the highest to the eigenvalue of $\hat{H}$ and hence decides the time increment for the numerical propagation of the wavefunction. In order to avoid the difficulties arising from these singularities, the grid was discretized in the range $\theta_{min} \leqslant \theta \leqslant \theta_{max}$, where $\theta_{min} = 0.23892$ and $\theta_{max} = 1.55859$ rad with $\Delta\theta = 0.04257$. The choice of θ_{min} was dictated by various factors. It had to be as small as possible in order to encompass the entire region of θ in which the wavefunction was being propagated. But we knew that the lowest energy of the symmetric top configuration $(\theta = 0)$ of HeH_2^+ was approximately 2 eV, and hence symmetric and near-symmetric top configurations would not be attained at energies much lower than that, validating the exclusion of $\theta = 0$ and nearby points in the present study. In addition, a value of θ_{min} close to zero would drastically increase the upper bound to the eigenvalue of the Hamiltonian and hence necessitate very small time increments for the numerical propagation of the wavefunction, making the computation prohibitively expensive.

The translational wave packet was centered at $\rho_0 = 8$ a.u. and was given a momentum corresponding to an $\langle E_{trans} \rangle$ of 1 eV. The time evolution of the wavefunction was carried out using the Chebyschev polynomial expansion of the evolution operator (Tal-Ezer and Kosloff 1984) and a three-point finite difference scheme for the spatial derivatives. The fast Fourier transform method was not used for the evaluation of the spatial derivatives as the wavefunction along θ was not periodic. To make it periodic along θ, we would have had to extend the θ grid to the range $\pi/2$ to π, thus doubling the storage and computational requirements.

3. Results and discussion

As a test case, for $v = 1$, $j = 0$ of H_2^+ at $\langle E_{trans} \rangle = 1$ eV, the wavefunction was propagated for 50 time steps with each time step $\Delta t = 5.38$ fs. The probability density distribution obtained in (θ, ϕ) space at the end of the time evolution for different values of $\rho = 4.66$, 6.06, 7.46 and 8.86 a.u. is illustrated in figure 2. It is evident from figure 2a for $\rho = 4.66$ a.u. that a significant portion of the wave packet is trapped in the interaction region. With increase in ρ, the coupling between the different channels becomes weaker, and the wavefunction begins to concentrate around the different asymptotic channel positions as can be seen from figures 2b–d. It is also clear from these plots that the wavefunction has not reached the θ_{min} boundary, and our choice of θ_{min} has not had any deleterious effect on the propagation of the wavefunction.

Due to the trapping of a significant portion of the final wavefunction in the interaction region, we could not adopt the usual method of projecting the final wavefunction onto different asymptotic (diatomic) vib-rotational states for obtaining state-resolved reaction probabilities. Such a procedure can be applied only if the wave function has completely moved out of the interaction region and well over into the different asymptotic channels. Temporal evolution till this is achieved would lead to problems arising from artificial interference due to reflection of the wavefunction from the large ρ boundary. But this can be circumvented by employing absorbing boundaries at large ρ values. In addition, it is possible to monitor the flux at a large
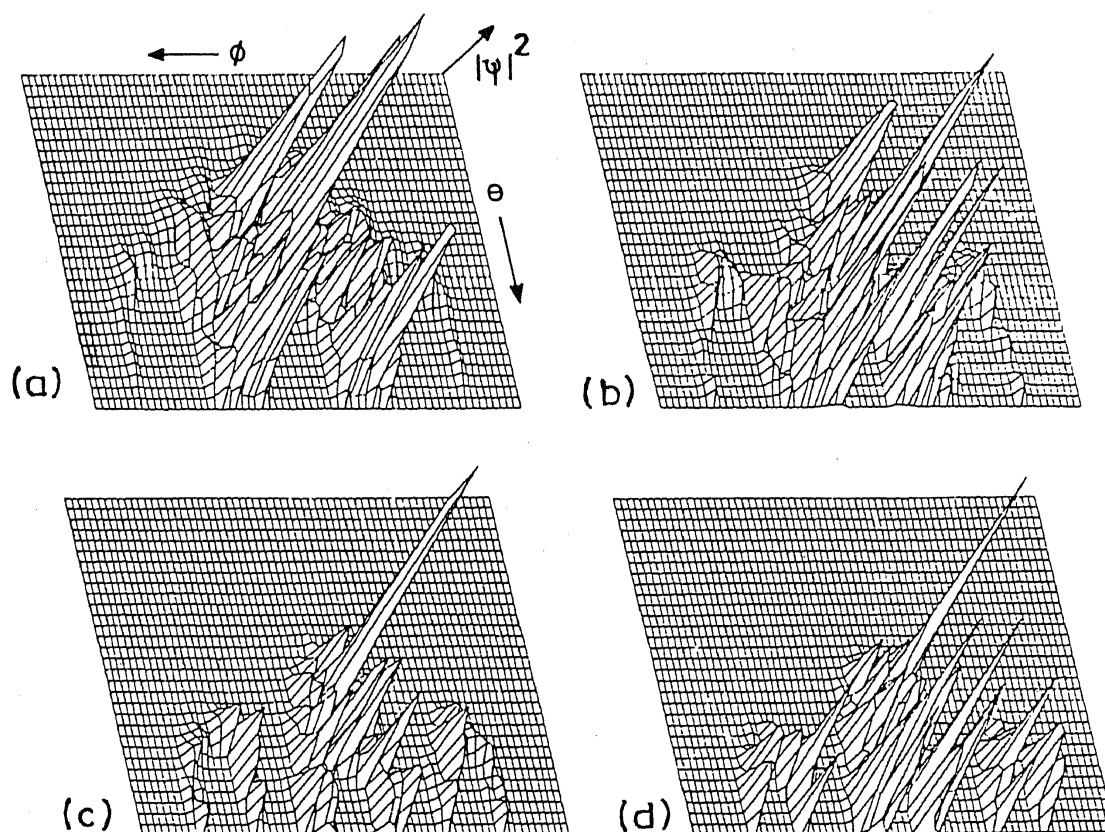
Figure 2. Plots of probability density as a function of θ and ϕ for fixed values of $\rho = 4\cdot66$, $6\cdot06$, $7\cdot46$ and $8\cdot86$ a.u. in (a)–(d) respectively, at the end of the time evolution for 50 time steps with each time step $= 5\cdot38$ fs, for $v = 1$ of H_2^+, $\langle E_{trans} \rangle = 1$ eV, the initial wavepacket centred at $\rho_0 = 8$ a.u.

ρ and determine the energy-resolved reaction probability by switching over to an E-representation (for example, see Marković and Billing 1992b). But as a first step we have computed the overall reaction probability by integrating numerically the probability density in the two $HeH^+ + H$ channels using the extended Simpson's rule. We hope to report on the E_{trans} dependence of state-to-state reaction probabilities in the near future.

Results for $v = 0$ and 1 given in table 1 show a clear vibrational enhancement of the reaction, in qualitative accord with the experimental (Chupka and Russel 1968;

Table 1. Average reaction probabilities $\langle P^R \rangle$ for $v = 0$ and 1 of H_2^+ ($j = 0$) at $\langle E_{trans} \rangle = 1$ eV for the wavepacket centred at $\rho_0 = 8$ a.u.

	$\langle P^R \rangle$		
v	Channel I	Channel II	Total $\langle P^R \rangle$
0	0·037	0·042	0·079
1	0·103	0·110	0·213

Chupka *et al* 1969; Chupka 1972; Paćak *et al* 1977; Turner *et al* 1984; van Pijkeren *et al* 1984; Govers and Guyon 1987; Achtenhagen *et al* 1991; Pollard *et al* 1991) and 3D quasiclassical trajectory (QCT) results (Kuntz and Whitten 1975; Whitten and Kuntz 1976; Joseph and Sathyamurthy 1984, 1987; Kumar and Sathyamurthy 1989, 1993). This is in striking contrast to the earlier time-independent (Kouri and Baer 1974; Adams 1975; Joseph and Sathyamurthy 1985; Sathyamurthy *et al* 1987) as well as time-dependent (Stroud *et al* 1977; Balakrishnan and Sathyamurthy 1991, 1993) quantum mechanical results for the reaction in collinear geometrices which did not reveal vibrational enhancement. Recent 3D time-independent quantal calculations (Kress *et al* 1990; Zhang *et al* 1990; Lepetit and Launay 1991) for the reaction have, however, revealed vibrational enhancement. Unfortunately, our results are not directly comparable to the 3D time-independent quantum mechanical (TIQM) results as the latter are highly energy-resolved and they reveal a large number of narrow reactive scattering resonances. In such situations, the standard practice (see, for example, Balakrishnan and Sathyamurthy 1991) is to obtain the energy-averaged result from the TIQM calculations and compare it with the TDQM result. Unfortunately, the TIQM results are available only over a limited range of E_{trans}. An indication of resonances in 3D dynamics is available from the complicated structures in the probability density plots. Furthermore, the fact that quite a bit of the probability density is confined to small ρ values at the end of the time evolution puts a lower bound on the lifetime of the collision complex: 0·27 ps, in accord with the estimates from the TIQM calculations. A more quantitative account of the complex formation will be reported subsequently. Already the present set of calculations took about 7 hours of cpu time for each choice of v and $\langle E_{trans} \rangle$ on our Convex C220.

We have also carried out a preliminary investigation of the isotopic exchange reaction

$$\text{He} + \text{HD}^+ \rightarrow \text{HeH}^+ + \text{D}; \ \text{HeD}^+ + \text{H}$$
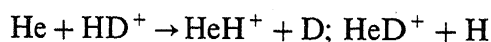
which is particularly relevant in the light of some discrepancies between experimental (Turner *et al* 1984) and 3D QCT calculations (Bhalla and Sathyamurthy 1989; Kumar *et al* 1993) for this reaction. For example, experiments showed that the isotopic branching ratio

$$\Gamma^{\text{E}} = \frac{\sigma^{\text{E}}(\text{HeH}^+)}{\sigma^{\text{E}}(\text{HeD}^+)}, \tag{7}$$

where σ^{E} is the exchange cross section for the appropriate channel, was an increasing function of v, for $v = 1\text{--}3$ of HD^+ at $E_{trans} = 1\,\text{eV}$, whereas the 3D QCT calculations showed that Γ^{E} remained approximately constant at about 0·9 for $v = 1\text{--}3$ (see table 2).

Grid parameters used in the TDQM calculations for HeHD^+ are the same as those used for HeH_2^+. The different asymptotic channel positions however are as follows: the $\text{He} + \text{HD}^+$ channel at $\phi = 180°$, the $\text{HeH}^+ + \text{D}$ channel at $\phi = 93·73°$ and the $\text{HeD}^+ + \text{H}$ channel at $\phi = 303·82°$. The results for $v = 1\text{--}3$ and $j = 0$ of HD^+, $\langle E_{trans} \rangle = 1\,\text{eV}$, in table 2 show a preferential HeD^+ formation with Γ^{E} being almost constant (0·5–0·6), in qualitative agreement with the QCT results. A more detailed study of the isotopic branching, especially the translational dependence of Γ^{E}, is being pursued further.

Table 2. Average reaction probabilities $\langle P^R \rangle$ and branching ratios Γ^E for $v = 1$, 2 and 3 of HD^+ $(j = 0)$, $\langle E_{trans} \rangle = 1.0\,eV$, for the isotopic branching in $HeHD^+$ obtained from 3D TDQM calculations using $\rho_0 = 8\,a.u.$ Γ^E values from 3D QCT calculations and experimental results are included for comparison.

	$\langle P^R \rangle$		Γ^E		
v	$HeH^+ + H$	$HeD^+ + H$	a	b	c
1	0·078	0·153	0·51	0·91	0·72
2	0·088	0·168	0·52	0·92	1·04
3	0·094	0·155	0·61	0·86	1·38

a – Present; b – 3D QCT (Bhalla and Sathyamurthy 1989); c – Experiment (Turner *et al* 1984).

4. Conclusion

Preliminary results of three-dimensional $(J = 0)$ time-dependent quantal calculations for He–H_2^+ $(v = 0, 1)$ collisions reproduce the vibrational enhancement known from experiments and 3D QCT calculations. TDQM calculations for He–HD^+ reveal a preferential HeD^+ formation over HeH^+, in accord with experiment and 3D QCT theory for $v = 1$ of HD^+. But with increase in v to 2 and 3, Γ^E obtained from the TDQM calculations remains approximately constant in contrast to the experiments, which suggest an increase in Γ^E.

Acknowledgement

References

Achtenhagen M, Schweizer M and Gerlich D 1991 (private communication)
Adams J T 1975 *Chem. Phys. Lett.* **33** 275
Balakrishnan N and Sathyamurthy N 1991 *Comput. Phys. Commun.* **63** 209
Balakrishnan N and Sathyamurthy N 1993 *Chem. Phys. Lett.* **201** 294
Bhalla K C and Sathyamurthy N 1989 *Chem. Phys. Lett.* **160** 437
Chupka W A 1972 in *Ion–molecule reactions* (ed.) J C Franklin (New York: Plenum) vol. 1, chap. 3, pp. 71–73
Chupka W A, Berkowitz J and Russel M E 1969 *Sixth international conference on physics of electronic and atomic collisions* (Cambridge Mass, USA: MIT Press), pp. 71–72
Chupka W A and Russel M E 1968 *J. Chem. Phys.* **49** 5426
Gerber R B, Kosloff R and Berman M 1986 *Comput. Phys. Rep.* **5** 59
Govers T R and Guyon P-M 1987 *Chem. Phys.* **113** 425
Johnson B R 1980 *J. Chem. Phys.* **73** 5051
Joseph T and Sathyamurthy N 1984 *J. Chem. Phys.* **80** 5332
Joseph T and Sathyamurthy N 1985 *J. Indian Chem. Soc.* **62** 874
Joseph T and Sathyamurthy N 1987 *J. Chem. Phys.* **86** 704
Judson R S, Kouri D J, Neuhauser D and Baer M 1990 *Phys. Rev.* **A42** 351

Kosloff R 1988 *J. Phys. Chem.* **92** 2087

Kouri D J and Baer M 1974 *Chem. Phys. Lett.* **24** 37

Kress J D, Walker R B and Hayes E F 1990 *J. Chem. Phys.* **93** 8085

Kulander K C (ed.) 1991 *Comput. Phys. Commun.* **63** 1–584 (thematic issue)

Kumar S and Sathyamurthy N 1989 *Chem. Phys.* **137** 25

Kumar S, Sathyamurthy N and Bhalla K C 1993 *J. Chem. Phys.* **98** 4680

Kuntz P J and Whitten W H 1975 *Chem. Phys. Lett.* **34** 340

Kuppermann A 1975 *Chem. Phys. Lett.* **32** 374

Lepetit B and Launay J M 1991 *J. Chem. Phys.* **95** 5159

Marković N and Billing G D 1992a *Chem. Phys. Lett.* **195** 53

Marković N and Billing G D 1992b *J. Chem. Phys.* **97** 8201

Marković N and Billing G D and Muckerman J T 1990 *Chem. Phys. Lett.* **172** 509

McLaughlin D R and Thompson D L 1979 *J. Chem. Phys.* **70** 2748

Mohan V and Sathyamurthy N 1988 *Comput. Phys. Rep.* **7** 213

Muckerman J T, Gilbert R D and Billing G D 1988 *J. Chem. Phys.* **88** 4779

Neuhauser D, Baer M, Judson R S and Kouri D J 1990 *J. Chem. Phys.* **93** 312

Pačak V, Havemann U, Herman Z, Schneider F and Zülicke L 1977 *Chem. Phys. Lett.* **49** 273

Pollard J E, Johnson L K and Cohen R B 1991a *J. Chem. Phys.* **95** 4894

Pollard J E, Syage J A, Johnson L K and Cohen R B 1991b *J. Chem. Phys.* **94** 8615

Sathyamurthy N, Baer M and Joseph T 1987 *Chem. Phys.* **114** 73

Smith F T 1962 *J. Math. Phys.* **3** 735

Stroud C, Sathyamurthy N, Rangarajan R and Raff L M 1977 *Chem. Phys. Lett.* **48** 350

Tal-Ezer H and Kosloff R 1984 *J. Chem. Phys.* **81** 3967

Turner T, Dutuit O and Lee Y T 1984 *J. Chem. Phys.* **81** 3475

van Pijkeren D, Boltjes E van Eck and Niehaus A 1984 *Chem. Phys.* **91** 293

Whitten W H and Kuntz P J 1976 *J. Chem. Phys.* **64** 3624

Whitten R C and Smith F T 1968 *J. Math. Phys.* **9** 1103

Zhang J Z H, Yeager D L and Miller W H 1990 *Chem. Phys. Lett.* **173** 489